PHYSICAL REVIEW A VOLUME 38, NUMBER 1 JULY 1, 1988

Multiconfiguration Hartree-Fock calculation of the photoionization of the excited Na 4*d* state

H. P. Saha
Department of Physics, University of Central Florida, Orlando, Florida 32816-0993
and Supercomputer Computations Research Institute, Florida State University, Tallahassee, Florida 32306-4052

M. S. Pindzola
Physics Division, Oak Ridge National Laboratory, Oak Ridge, Tennessee 37831

R. N. Compton
Chemical Physics Section, Health and Safety Research Division, Oak Ridge National Laboratory, Oak Ridge, Tennessee 37813-6125

(Received 12 November 1987)

The photoionization cross section for the excited Na 4*d* state has been calculated with the multiconfiguration Hartree-Fock method. *Ab initio* methods are used to take into account the core-polarization effects. The minimum (zero) in the $4d \rightarrow kp$ cross section has been calculated and it is found that including the effects of core-polarization shifts the position of the minimum (zero) to a higher energy. The calculation of the photoionization angular distribution asymmetry parameter is an excellent test to locate the minimum (zero) in the cross section. The present results are in good agreement with the experimental results of Smith *et al.* [Phys. Rev. A **22**, 577 (1980)] performed at a single photon energy.

I. INTRODUCTION

The study of photoionization of excited states of atoms offers an opportunity to investigate the ionization process from a given state of total energy, angular momentum, and alignment. Excited-state photoionization is of importance in controlled thermonuclear research plasmas and in regions of high temperature, such as stellar atmospheres. This type of process is also useful in understanding radiative recombination, the inverse process.

The study of photoionization of excited states of atoms is of considerable current interest. A few cross sections for excited alkali-metal atoms have been reported.[1–11] There are many more studies of resonantly enhanced multiphoton ionization (REMPI). In some experiments, REMPI can be described as one-or-more-photon ionization of an excited state (see, for example, Dodhy *et al.*,[12] and others cited therein). Comparing the theory with many of these measurements is complicated by experimental problems, such as the lack of knowledge of the alignment of the excited atoms or polarization of the ionizing radiation, hyperfine or fine-structure coupling effects of the excited state, and saturation of the ground-to-excited-state transition. Smith *et al.*[9] overcame most of these problems and determined the photoionization cross section for 4*d* and 5*s* excited sodium atoms. Furthermore, these authors used linearly and circularly polarized light to obtain a partial cross section for photoionization of 4*d* Na atoms into the *kp* and *kf* continua at the frequency of the fundamental of the Nd: yttrium aluminum garnet (YAG) laser (1064 nm) corresponding to a photon energy of 0.086 Ry.

The existence of so-called Cooper minima[13,14] in photoionization cross sections has been known for a long time. They generally occur in the photoionization of outer *nl* electrons, provided the discrete *nl* wave function has at least one node. Minima arise when the matrix element vanishes as a result of the equality of the positive and the negative contributions to the dipole matrix element. Over the past decade, theoretical work[15–17] on the photoionization cross sections of excited states of atoms has predicted that zeros in the dipole matrix element are much more widespread than for ground-state photoionization. Recently, it has been predicted that for excited-state photoionization, zeros can occur in the $l \rightarrow l-1$ transition.[15–18] One experimental test of the theoretical calculations was unsuccessful. Specifically, the deep minimum in the photoionization cross section for the $6\,^2D_{3/2}$ state of cesium by Manson and Cooper[14] and Msezane and Manson[15] was not verified experimentally by Gerwert and Kollath.[10] In fact, there is very little experimental work on excited-state photoionization cross sections, and even less which covers a significant energy range.[11] Experimental data for a wide range of energies are of great importance for assessing the accuracy of the theoretical work. Cross sections at a single photon energy, although useful, are not sufficient for verification of the theoretical results. Smith *et al.*[9] measured the absolute cross section for the photoionization of the 4*d* excited states of sodium at a single photon energy of 0.086 Ry. Their method of measurement is based on saturation of ionization probability at high intensity of the incoming radiation. They obtained photoionization cross sections of 15.2±1.7 Mb for the $4d \rightarrow kf$ transition and less than 0.10 Mb for the $4d \rightarrow kp$ transition; the latter was too small to be seen in the experiment.

Recently, Msezane *et al.*[19] reported results for the photoionization cross section of the excited 4*d* state of atomic sodium in the Hartree-Fock (HF) approximation. The HF calculations predict a zero in the $l \rightarrow l-1$ photoionization cross section. The experimental value[9] for this transition is less than 0.10 Mb, and it is not clear where the actual zero of the cross section lies. The HF calculation of Msezane *et al.*[19] indicates that a zero exists in the general vicinity of the experimental point (upper limit). The effects of electron-electron correlation and the dipole core-polarization effects are specifically neglected in the HF calculation and are expected to have an appreciable effect on the photoionization cross section of the excited Na 4*d* state. It is of interest to have more accurate calculations beyond the HF approximation in order to give accurate predictions of minima in the $4d \rightarrow kp$ partial cross section.

The purpose of this paper is to investigate the behavior of the photoionization cross section for the excited-state Na 4*d* by performing calculations in the multiconfiguration Hartree-Fock (MCHF) approximation.[20,21] The emphasis in this study is to take into account of the dynamical core polarization effect *ab initio*. Previous calculations[20,21] of photoionization cross sections using the MCHF procedure were found to be very accurate.

The calculations have been performed using both the simple HF and the more sophisticated MCHF wave functions for the initial excited discrete state and the final continuum state. Recently, the MCHF method has been applied favorably well to the study of photoionization cross sections of the ground state of atomic sodium.[20] In this paper we report a similar study of core-polarization effects in the photoionization cross section of the excited 4*d* state of a sodium atom. As mentioned in our previous paper,[20] the MCHF program generally used for the bound-state calculation has been extended to compute the MCHF continuum wave functions. This program is capable of simultaneously varying the bound and the continuum orbitals to take into account the dynamical core-polarization effect very accurately.

II. THEORY

A. Photoionization cross sections

The photoionization cross section for a transition from an initial state *i* to a final state *f* is given by

$$\sigma(\omega)=4\pi^2\alpha a_0^2\omega \sum_{f,m} |\langle \Psi_f | T | \Psi_i \rangle|^2 ,$$

where the dipole transition operator T is given by

$$T=T_L=\sum_{j=1}^{n} Z_j$$

in the length form and

$$T=T_V=\sum_{j=1}^{n} \frac{\nabla_j^z}{i\omega}$$

in the velocity form. The matrix elements

$$M=\langle \Psi_f | T | \Psi_i \rangle$$

are evaluated in a.u., ω is the energy of the incident photon in a.u., α is the fine-structure constant, and a_0 is the Bohr radius of the hydrogen atom. Ψ_i and Ψ_f are the initial- and the final-state wave functions, respectively, and the sums run over final configurations and all magnetic quantum numbers. The length and the velocity forms of the cross sections will be identical when Ψ_i and Ψ_f are exact solutions of the same Hamiltonian.

B. Asymmetry parameter $\beta_{nl}(\omega)$

The study of the angular distribution of electrons relative to the incident photon and/or polarization direction is a very powerful tool in extracting and separating geometrical and dynamical factors involved in the photoionization process. The angular distribution of photoelectrons ionized from a particular subshell *nl* by light polarized in the $\hat{\mathbf{e}}$ direction is related to the differential cross section for photoionization at energy ω by the relation[22]

$$\frac{d\sigma_{nl}(\omega)}{d\Omega}=\frac{\sigma_{nl}(\omega)}{4\pi}[1+\beta_{nl}(\omega)P_2(\hat{\mathbf{e}}\cdot\hat{\mathbf{k}})] ,$$

where $\sigma_{nl}(\omega)$ is the total photoionization cross section at energy ω corresponding to the electron ionized from the subshell *nl*. P_2 is the second-order Legendre polynomial, whose argument is the cosine of the angle between the polarization vector $\hat{\mathbf{e}}$ of the incident radiation and the direction $\hat{\mathbf{k}}$ of the photoelectron momentum, and $d\Omega$ is the solid angle into which the photoelectron is scattered. The quantity $\beta_{nl}(\omega)$ is the asymmetry parameter, which is a function of ω, because of interference between various final states of the ion plus photoelectron. The parameter $\beta_{nl}(\omega)$ is more sensitive to the behavior of the photoionization amplitude than the total or even the partial cross sections.

In the Cooper-Zare model, the asymmetry parameter $\beta_{nl}(\omega)$ is given by[23]

$$\beta_{nl}(\omega)=\frac{l(l-1)T_{l-1}^2(\omega)+(l+1)(l+2)T_{l+1}^2(\omega)-6l(l+1)T_{l-1}(\omega)T_{l+1}(\omega)\cos(\xi_{l+1}-\xi_{l-1})}{(2l+1)[lT_{l-1}^2(\omega)+(l+1)T_{l+1}^2(\omega)]} ,$$

where $T_{l-1}(\omega)$ and $T_{l+1}(\omega)$ are the radial parts of the dipole matrix element corresponding to the $l-1$ and $l+1$ channels, respectively, and $\xi_l(\omega)$ is the total phase shift of the lth channel.

C. MCHF wave function for the continuum state

The MCHF wave function for a continuum state with label λ, energy E, and term LS may be expressed in a series of the form

$$\Psi(\gamma LS;N+1)=\sum_{j}^{m_c} a_j\Phi(\gamma_j L_c S_c;N)\phi_{kl} + \sum_{i}^{m} c_i\Phi(\gamma_i LS;N+1) \ ,$$

where the first term represents the coupling of a wave function describing an N-electron core that is an eigenstate of L_c and S_c, in terms of an N-electron bound configuration state $\Phi(\gamma_j L_c S_c;N)$ with configuration γ_j and term L_cS_c, mixing coefficients a_j, and the total energy E_c, with a single electron continuum orbital to yield an antisymmetric configuration state for the $(N+1)$-electron system with the designated final term value and configuration $\gamma_j kl$. The MCHF method for continuum states assumes that all the radial functions describing the core are fixed along with the mixing coefficients a_j. Other bound-state radial functions may be determined variationally along with the radial function for the continuum electron. In the close-coupling approximation, all the radial functions are solutions of the equations of the form

$$\left[\frac{d^2}{dr^2}+\frac{2Z}{r}-\frac{l(l+1)}{r^2}\right]P_i(r) =\frac{2}{r}[Y_i(r)P_i(r)+X_i(r)+I_i(r)]+\sum_{i'}\varepsilon_{ii'}P_{i'}(r) \ ,$$

where the off-diagonal energy parameters $\varepsilon_{ii'}$ are related to Lagrange multipliers that ensure orthogonality assumptions. Here $(2/r)Y_i(r)$ is the screening potential, $(2/r)X_i(r)$ is the exchange function, and $(2/r)I_i(r)$ represents terms arising from interactions between configuration states (for a detailed discussion of these equations for bound state systems see Ref. 24). The boundary conditions satisfied by the bound radial functions are

$$P_i(r)\xrightarrow[r\to 0]{} r^{l+1}, \quad P_i(r)\xrightarrow[r\to\infty]{} 0 \ .$$

In this case the diagonal energy parameter ε_{ii} must be an eigenvalue of the integrodifferential equation for nontrivial solutions to exist and hence needs to be determined. The radial function for the continuum orbital satisfies the conditions

$$P_i(r)\xrightarrow[r\to 0]{} r^{l+1} \ ,$$

$$P_i(r)\xrightarrow[r\to\infty]{} \left[\frac{2}{\pi k}\right]^{1/2} \sin[kr-l\pi/2+(q/k)\ln(2kr) +\sigma_l+\delta_l] \ ,$$

where $\sigma_l=\arg[\Gamma(l+1-iq/k)]$ is the Coulomb phase shift, $q=Z-N$ is the net charge of the ion, and $\varepsilon_{ii}=-k^2$, k^2 being the kinetic energy of the photoelectron. The coefficients c_i are solutions of the system of equations

$$\sum_{i'}^{m}\langle\Phi_i\,|\,H-E\,|\,\Phi_{i'}\rangle c_{i'}+\sum_{j}^{m_c}\langle\Phi_i\,|\,H-E\,|\,\Phi_j\rangle a_j=0 \ , \qquad i=1,\ldots,m$$

where

$$\Phi_j=\Phi(\gamma_j L_c S_c;N)\phi_{kl}, \quad j=1,\ldots,m_c$$

and

$$\Phi_i=\Phi(\gamma_i LS;N+1), \quad i=1,\ldots,m \ .$$

III. COMPUTATIONAL PROCEDURE

We consider the processes

$$h\nu+\mathrm{Na}(2s^22p^64d\ ^2D)\rightarrow\mathrm{Na}^+(2s^22p^6\ ^1S)+e^-(kp)\ ^2P^0$$
$$\rightarrow\mathrm{Na}^+(2s^22p^6\ ^1S)+e^-(kf)\ ^2F^0 \ .$$

As stated earlier, the electron-electron correlation and the dynamical core-polarization effects are very important on the photoionization cross section of the excited Na $4d$ state. To study the effect of core polarization by the valence electron in the initial state and by the continuum electron in the final state, two sets of calculations are performed. In the HF calculation, which neglects the electron correlation and the polarization effects, both the initial and the final states are represented by the single configuration. In the MCHF calculation, which considers the correlation and polarization effects very accurately, all the configurations contributing to the core polarization are included. The main emphasis in this study is to take into account the dynamical core-polarization effect *ab initio.* To simplify the evaluation of the electric dipole transition matrix elements, the $1s$, $2s$, and $2p$ radial functions for both the states are obtained from the HF calculation of the $2p^64d\ ^2D$ state.

A. Initial-state wave function: $2p^64d\ ^2D$

The MCHF wave-function expansion for the initial-state wave function is over the set of 71 configuration states coupled to form a ^2D term,

$$\{2s^22p^64d, 2s^22p^53s3p, 2s^22p^53p3d, 2s^22p^63d, 2s^22p^53p4s, 2s^22p^53p4d, 2s^22p^53s4p, 2s^22p^53s4f \ ,$$
$$2s^22p^53d4p, 2s^22p^53d4f, 2s^22p^54s4p, 2s^22p^54s4f, 2s^22p^54p4d, 2s^22p^54d4f, 2s2p^63s3d, 2s2p^63d^2 \ ,$$
$$2s2p^63d4s, 2s2p^63d4d, 2s2p^63s4d, 2s2p^63p4p, 2s2p^63p4f, 2s2p^64s4d, 2s2p^64p4f, 2s2p^63p^2 \ ,$$
$$2s2p^64p^2, 2s2p^64d^2, 2s2p^64f^2\}\ ^2D \ .$$

The initial-state radial functions were obtained by the MCHF calculation varying seven bound orbitals simultaneously. In this initial-state expansion it is found that the configurations $2s^22p^53d4f$, $2s^22p^53s4f$, $2s^22p^53s3p$, and $2s^22p^53p3d$ are very important.

B. Final-state wave functions

1. $2p^6kp\ {}^2P^\circ$

The final MCHF continuum wave-function expansion for the $2p^6kp\ {}^2P^\circ$ state is over the 58 configurations coupled to form a ${}^2P^\circ$ term,

$$\begin{gathered}\{2s^22p^6kp_1, 2s^22p^53p_2^2, 2s^22p^54p_2^2, 2s^22p^53s^2, 2s^22p^53s3d, 2s^22p^53s4s, 2s^22p^53s4d\ , \\ 2s^22p^53p_24f, 2s^22p^53d4s, 2s^22p^53d4d, 2s^22p^54s4d, 2s^22p^54p_24f, 2s^22p^53d^2, 2s^22p^54s^2\ , \\ 2s^22p^54d^2, 2s^22p^54f^2, 2s2p^63s3p_2, 2s2p^63p_23d, 2s2p^63p_24s, 2s2p^63p_24d, 2s2p^63s4p_2\ , \\ 2s2p^63d4p_2, 2s2p^63d4f, 2s2p^64s4p_2, 2s2p^64p_24d, 2s2p^64d4f\}\ {}^2P^\circ\ .\end{gathered}$$

The radial functions $3s$, $3p_2$, $3d$, $4s$, $4p_2$, $4d$, $4f$, and kp_1 are varied simultaneously for each kinetic energy of the photoelectron.

2. $2p^6kf\ {}^2F^\circ$

For the final continuum state $2p^6kf\ {}^2F^\circ$, the MCHF expansion was over the set of 104 configuration states,

$$\begin{gathered}\{2s^22p^6kf_1, 2s^22p^53s3d, 2s^22p^53s4d, 2s^22p^53s5d, 2s^22p^53s5g, 2s^22p^53s6g, 2s^22p^53d4s\ , \\ 2s^22p^53d4d, 2s^22p^53d5d, 2s^22p^53d5g, 2s^22p^53d6g, 2s^22p^54s4d, 2s^22p^54s5d, 2s^22p^54s5g\ , \\ 2s^22p^54s6g, 2s^22p^54d5d, 2s^22p^54d5g, 2s^22p^54d6g, 2s^22p^55d5g, 2s^22p^55d6g, 2s^22p^63d^2\ , \\ 2s^22p^54d^2, 2s^22p^55d^2, 2s2p^63p3d, 2s2p^63d4p, 2s2p^63p4d, 2s2p^63p5d, 2s2p^63p5g, 2s2p^63p6g\ , \\ 2s2p^64p4d, 2s2p^64p4d, 2s2p^64p5g, 2s2p^64p6g\}\ {}^2F^\circ\ .\end{gathered}$$

In this expansion ten radial functions, $3s$, $3p$, $3d$, $4s$, $4p$, $4d$, $5d$, $5g$, $6g$, and kf_1, were varied simultaneously for each kinetic energy of the photoelectron. In all cases, $1s$, $2s$, and $2p$ wave functions were kept fixed at the HF $2p^64d\ {}^2D$ value. In both of the final states, the excited-state configurations $2s^22p^53s3d$, $2s^22p^53d4s$, $2s^22p^53d4d$, and $2s^22p^53d^2$ are found to be very important in the calculation of the continuum wave functions.

IV. RESULTS

A. Continuum wave function

Two different approximations are used to compute the final-state continuum wave function. The first is the Hartree-Fock (HF) approximation, where the continuum wave function was calculated in the field of the HF core $2s^22p^6$. The $1s$, $2s$, and $2p$ wave functions of the core are taken from the HF calculation of the initial bound state $2p^64d$. In the correlated approximation, a large number of configurations are added to take into account the electron correlation and the polarization effects accurately *ab initio*. The continuum wave function is then calculated in the MCHF approximation. Near the origin, the differences in the continuum wave functions calculated in the two approximations are found to be very small. As the radius increases, the differences increase. Continuum wave functions for energies $k^2=0.10$ and 1.00 Ry show similar behavior. The phase shifts of the continuum wave functions in the two approximations change by 2.63%, 2.70%, and 3.27% for energies of 0.01, 0.10, and 1.0, respectively. It is also found that the change of energy of the correlated core does not change the wave function considerably.

Electric dipole matrix elements, photoionization cross sections, and photoelectron angular distribution asymmetry parameters were calculated in the length and the velocity forms using both the HF and the correlated wave functions.

B. Electric dipole matrix elements

In Fig. 1, the dipole matrix elements for the $4d \rightarrow kp$ transition in the length and the velocity forms are presented as a function of the photoelectron energy, using the HF and the correlated wave functions. The HF dipole matrix element in the length form shows zero at 0.035 Ry photoelectron energy, whereas the velocity dipole matrix element shows zero at slightly lower energy 0.030 Ry. In the HF approximation, the dipole matrix element in the length form reaches maximum at about 0.125 Ry, whereas the velocity dipole matrix element goes to maximum at about 0.25 Ry. The correlated-length dipole matrix element behaves in a manner similar to that of the HF-length dipole matrix element, but reaches zero between 0.065 and 0.070 Ry, and reaches maximum at about 0.175 Ry. On the other hand, the velocity dipole matrix element shows a behavior similar to that of the HF-velocity dipole matrix element, but goes to zero between 0.065 and 0.070 Ry and then increases up to 0.35 Ry and then slowly decreases. From the figure it is found that the correlated results which are considered to be more accurate show zero at a higher energy than that of the HF result. This shifting of zero to a higher energy is due to the effect of dynamical core polarization.

The dipole matrix elements for the $4d \rightarrow kf$ transition

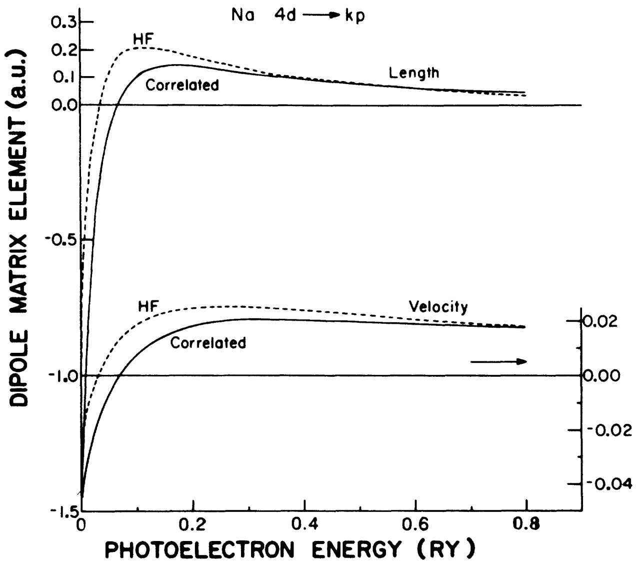

FIG. 1. Dipole matrix element for the Na $4d \rightarrow kp$ transition as a function of photoelectron energy (Ry), using Hartree-Fock and correlated (MCHF) wave functions in both length and velocity formulations.

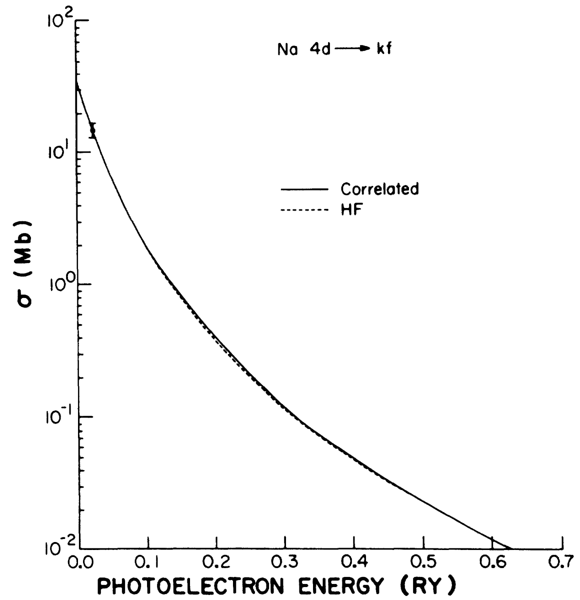

FIG. 2. Partial Na $4d \rightarrow kf$ photoionization cross section as a function of photoelectron energy (Ry) using Hartree-Fock (HF) and the correlated (MCHF) wave functions.

have also been calculated using both the HF and the correlated wave functions. These are not shown in Fig. 1. In this case, the dipole matrix elements decrease monotonically from threshold to higher energy.

C. Photoionization cross sections

The multiconfiguration Hartree-Fock method is used to calculate the photoionization threshold of the Na $4d$ state. The calculated photoionization threshold of the Na $4d$ state is 0.8546 eV, which compares well to the experimental value of 0.8554 eV. Experimental threshold energies were used in both the HF and the correlated calculations.

The photoionization cross section for the $4d \rightarrow kf$ transition are shown in Fig. 2. Both the HF and the correlated results are plotted as a function of photoelectron energy. Length and velocity results in each of the approximations are in excellent agreement. This is why we simply plotted the length results in the two approximations. The present HF results for this transition are in good agreement with the HF results of Msezane *et al.*[19] From this figure it is seen that the HF results in this case are very close to but slightly smaller than the correlated results. It appears that the effect of dipole polarization is very small for this transition. The experimental cross section obtained by Smith *et al.*[9] at one photon energy agrees very well for this transition. The threshold value of the cross section is the same as the hydrogenic value of 35 Mb. This means that the $4d \rightarrow kf$ dipole matrix element, in the energy region of interest, is essentially hydrogenic.

In Fig. 3, the photoionization cross sections for the $4d \rightarrow kp$ transition are shown. Both the HF and the correlated length and velocity results are presented as a function of photoelectron energy. The HF length and velocity results decrease very sharply, then go to zero at about 0.035 and 0.030 Ry, respectively, then increase up to 0.150 Ry and then decrease. The HF results for this transition obtained by Msezane *et al.* agree very well with the present HF results, except for minor differences due to the different numerical method used to compute the HF continuum wave function. The correlated-length

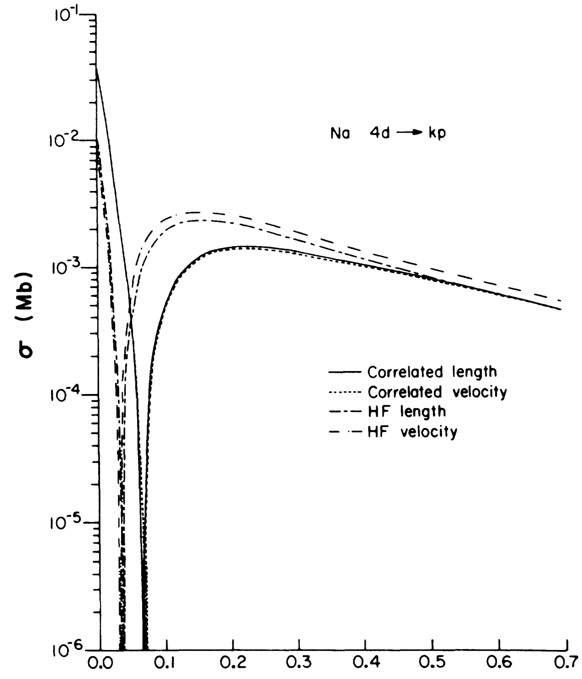

FIG. 3. Partial Na $4d \rightarrow kp$ photoionization cross section as a function of photoelectron energy (Ry), using Hartree-Fock (HF) and correlated wave functions in both length and velocity formulations.

and -velocity results show similar behavior. Both the cross sections reach zero between 0.065 and 0.070 Ry. The length and velocity results are in excellent agreement. The correlated results reach zero at a higher energy than the HF results. This shifting of the zero towards the higher energy is due to the effect of core polarization. Although both the HF and the correlated results agree with the experimental cross section (<0.1 Mb) at the single experimental energy, it is not clear where the actual zero exists.

D. Asymmetry parameter $\beta_{nl}(\omega)$

The asymmetry parameter $\beta_{nl}(\omega)$ for the Na 4*d* photoionization is shown in Fig. 4, where the HF and the correlated results are plotted as a function of photoelectron energy. From the expression of $\beta_{nl}(\omega)$, it is seen that at the point where the $4d \rightarrow kp$ cross section is zero, the photoionization electron angular distribution asymmetry parameter $\beta_{nl}(\omega)$ must be equal to 0.8. The asymmetry parameter $\beta_{nl}(\omega)$ depends on the accuracy of the phase shift. From Fig. 4 it is seen that HF-length and -velocity results reach a minimum value of 0.8 Ry between 0.03 and 0.035 Ry. In the neighborhood of zero, the HF-length and -velocity results are very close to each other. The correlated-length and -velocity results are nearly the same. In Fig. 4 we have shown the correlated-length results. Correlated results show similar behavior. They reach a minimum value 0.8 between 0.065 and 0.070 Ry, at which the cross section goes to zero as indicated earlier. The difference between the HF and the correlated results is due to the effect of core polarization.

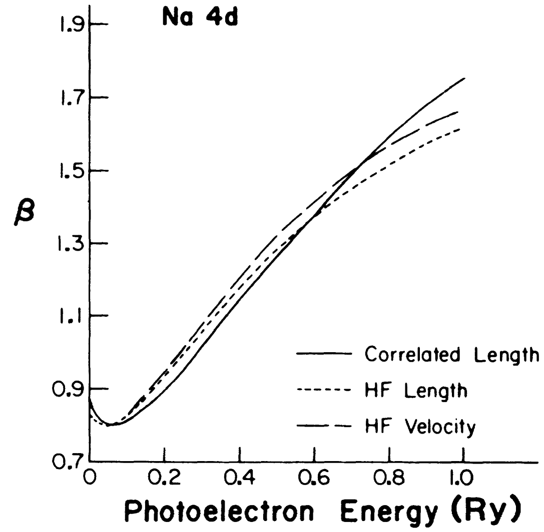

FIG. 4. Photoelectron angular distribution asymmetry parameter β for Na 4*d* in both length and velocity formulations, using Hartree-Fock (HF) and correlated (MCHF) wave functions.

V. CONCLUSION

The multiconfiguration Hartree-Fock method has been applied to calculate the photoionization cross section for the Na 4*d* excited state. The dynamical core-polarization effect, which is important in this case, has been taken into account very accurately in the *ab initio* calculation through the configuration interaction procedure. The existence of zero in the $4d \rightarrow kp$ excited-state photoionization cross section has been found at 0.0675 Ry. Near the zero the calculation becomes very sensitive. It has been found that the inclusion of core polarization dramatically changes the location of the zero in the cross section of the $4d \rightarrow kp$ transition. The position of the zero could also be inferred from the behavior of the photoelectron angular distribution asymmetry parameter $\beta_{nl}(\omega)$, as already indicated. Experimental results of Smith *et al.*,[9] performed at a single photon energy, agree well with the calculated results. At present there are no experimental results over a range of energies. Experimental measurement over a larger energy range would be extremely desirable.

ACKNOWLEDGMENTS

This research was supported by the grants from the U.S. Department of Energy (Contract No. DE-FC05-85 ER 250000) and in part by the Florida State University through time granted on its CYBER 205 supercomputer. R.N.C. was supported by Martin Marietta Energy Systems Inc., with the U.S. Department of Energy, under Contract No. DE-AC05-84OR21400.

---

[1] U. Heinzmann, D. Schinkowski, and H. D. Zeman, Appl. Phys. **12**, 113 (1977).

[2] R. V. Ambartzumian, N. P. Furzikov, V. S. Letokhov, and A. A. Puretsky, Appl. Phys. **9**, 335 (1976).

[3] D. E. Rothe, J. Quant. Spectrosc. Radiat. Transfer **11**, 355 (1971); **9**, 49 (1969).

[4] N. V. Karlov, B. B. Krynetskii, and O. M. Stel'makh, Kvant. Electron. (Moscow) **4**, 2275 (1977) [Sov. J. Quantum Electron. **7**, 1305 (1977)].

[5] A. N. Klyucharev and N. S. Ryazanov, Opt. Spektrosk. **32**, 1253 (1972) [Opt. Spectrosc. (USSR) **32**, 686 (1972)].

[6] A. N. Klyucharev and V. Yu. Sepman, Opt. Spektrosk. **38**, 1230 (1975) [Opt. Spectrosc. (USSR) **38**, 712 (1975)].

[7] V. P. Bolik, S. V. Bobashov, and L. A. Shmaenok, Pis'ma Zh. Eksp. Teor. Fiz. **25**, 527 (1977) [JETP Lett. **25**, 494 (1977)].

[8] R. F. Stebbings, F. B. Dunning, and R. D. Rundel, in *Atomic Physics*, edited by G. Zu Putlitz *et al.* (Plenum, New York, 1975), Vol. 4.

[9] A. V. Smith, J. E. M. Goldsmith, D. E. Nitz, and S. J. Smith, Phys. Rev. A **22**, 577 (1980).

[10] K. Gewert and K. J. Kollath, J. Phys. B **16**, L217 (1983).

[11] J. M. Preses, C. E. Burkhardt, R. L. Corey, D. L. Earsom, T. L. Daulton, W. P. Garver, J. J. Leventhal, A. Z. Msezane, and S. T. Manson, Phys. Rev. A **32**, 1264 (1985).

[12] A. Dodhy, J. A. D. Stockdale, R. N. Compton, X. Tang, P. Lambropoulos, and A. Lyras, Phys. Rev. A **35**, 2878 (1987).

[13] J. W. Cooper, Phys. Rev. **128**, 681 (1962).

[14] S. T. Manson and J. W. Cooper, Phys. Rev. **165**, 126 (1968).

[15] A. Z. Msezane and S. T. Manson, Phys. Rev. Lett. **35**, 364 (1975).

[16] A. Z. Msezane and S. T. Manson, Phys. Rev. Lett. **48**, 473 (1982).

[17] J. Lahiri and S. T. Manson, Phys. Rev. Lett. **48**, 614 (1982).

[18] N. B. Avdonina and M. Ya. Amusia, J. Phys. B **16**, L543 (1983).

[19] A. Z. Msezane, J. Lahiri, and S. T. Manson, Phys. Rev. A **33**, 4406 (1986).

[20] H. P. Saha, C. F. Fischer, and P. W. Langhoff, Phys. Rev. A (to be published).

[21] C. F. Fischer and H. P. Saha, Can. J. Phys. **65**, 772 (1987).

[22] C. N. Yang, Phys. Rev. **74**, 764 (1948).

[23] J. Cooper and R. N. Zare, in *Lectures in Theoretical Physics,* edited by S. Geltman, K. Mahathappa, and W. Britten (Gordon and Breach, New York, 1969), Vol. 11c, pp. 317–337.

[24] C. F. Fischer, Comput. Phys. Rep. **3**, 273 (1986).